IEEE Transactions on Nuclear Science, Vol. NS-28, No. 3, June 1981

PARTICLE BEAM FUSION ACCELERATOR-I (PBFA-I)

T. H. Martin, J. P. VanDevender, G. W. Barr, S. A. Goldstein, R. A. White, and J. F. Seamen
Sandia National Laboratories
Albuquerque, New Mexico 87185

Summary

The first Particle Beam Fusion Accelerator (PBFA-I) has recently completed its operational series of tests. It provided 30 TW into 36 power flow lines terminated in electron beam loads at the accelerator's center. The outputs were 2 MV at 15 MA for a 40 ns pulse which provided 1 MJ of output energy. During the accelerator development, several ways of modifying and reconnecting this modular, few MV output pulsed power were discovered. The data from PBFA-I tests show the flexibility and reliability of pulsed power. This technology base could provide a 100 TW accelerator known as PBFA-II which will be the light ion beam test bed for breakeven experiments for the Department of Energy's Inertial Confinement Fusion Program.

Pulsed power technology continues to be flexible and adaptable to a wide variety of basic research problems. It is a cost effective technology for producing large pulsed energy outputs.

Introduction

Inertial confinement fusion (ICF) breakeven targets require the focusing and delivery of a few megajoules of ion beam energy on target at a power of approximately 100 TW. In order to provide the electrical pulsed power to drive the ion diodes, a new generation of modular pulsed power accelerators has been developed. This pulsed power development has recently been demonstrated by the Particle Beam Fusion Accelerator-I (PBFA-I) during its operational series of tests where 30 TW and 1 MJ were provided into 36 power flow lines terminated in electron beam loads. A description of the accelerator, the test results and the implications of the technology will be presented.

Description of the PBFA-I Accelerator

The PBFA-I accelerator, shown in Figure 1, is contained in a tank that is 30.5 meters in diameter and 4.3 meters deep which is radially partitioned into three annular sections. The outermost annulus, 4.0 m wide, houses the Marx generators which are insulated with transformer oil during operation. The second annular chamber contains the water insulated capacitors, trigatrons and trigger lines, pulse forming lines, water switches, transmission lines, and vacuum interfaces. Hardware in the oil and water tanks are electrically connected through the barrier wall by means of 1.4 m diameter polyurethane insulating interfaces. The third tank section contains the vacuum insulated transmission lines, vacuum pumps, and central target chamber. No dielectric fluids other than ambient air are contained in the third section.

Thirty-six separate Marx generators provide the energy for thirty-six separate modules in the PBFA-I accelerator. Each Marx generator stores 112 kJ of energy at a maximum charge voltage of ± 100 kV on each of its thirty-two, 0.7 ufd, 100 kV capacitors. When the Marx is triggered, the capacitors are completely connected in series within 200 nsec. Next,

*This work supported by the U. S. Department of Energy under contract DE-AC04-76-DP00789.

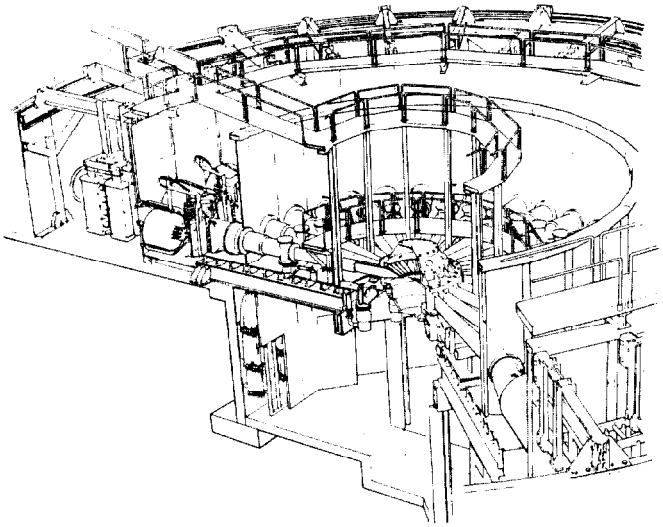

Figure 1. PBFA-I.

the Marx energy is transferred through the oil-water, high voltage interface in 750 nsec ($\pi\sqrt{LC}$) into the water capacitor. The 22 nfd water capacitor is charged to 2.5 MV, when the trigatron switch is initiated by means of a high voltage trigger pulse from the coax cable contained within the inductor coil. The inductor coil provides high voltage pulse isolation for the water section after the trigatron conducts current. Each water capacitor transfers its energy in 280 ns to two pulse forming lines; each of which has five self-breaking, water insulated switches. When the water switches break down due to overvolting, the energy is converted into a wave traveling within the water insulated transmission lines. The transmission lines deliver this pulse at 2 MV through the vacuum interface into the vacuum magnetically insulated transmission line (MITL). The pulse travels along the 6 m long MITL at a nominal field of 2 MV/cm and arrives at the central chamber where it is converted to individual particle beams or combined in magnetically insulated convolutes to provide a single pulse output. A magnetically insulated convolute is an abrupt mechanical change in the MITL's output to allow them to be interconnected for driving the same load. A balance between the electric and magnetic fields is required for efficient operation. Presently, an experiment connecting several MITL's is underway.

Marx Generator Test Results

The Marx generators[1] are triggered by a 400 kV, fast rise (~ 20 ns) pulse from the Maxwell Laboratories (PortaMarx) trigger generators. The overall Marx output spread, which is defined as the time between first-to-last Marx output, ranged from 15 ns to 25 ns which indicates the rms standard deviation of the Marx generator timing is between 4 and 6 ns. A Marx prefire, which is defined as an untriggered Marx breakdown before a test shot, occurred frequently during the initial testing. Many operational procedures and component problems cause prefires. Problems such as bubbles in the copper sulphate charging resistors, capacitor failure, oil vapor or debris contaminating the spark gaps, or Marx charging

supply disconnect transients have all caused prefires. Stringent controls of the Marx maintenance procedures and of the charging and firing system have alleviated these problems. We have found 24 prefires out of a total of 1700 total Marx generator chargings. After discounting 16 of these prefires which were caused by the same faulty capacitor, then the overall prefire rate is 0.0053 per Marx charging cycle. If all of the remaining failures are attributed to the Marx spark gaps, we calculate that the Marx spark gap reliability exceeds 0.9996. Our present expectation for a single, successful, non-prefire PBFA-I test cycle is 0.82.

Water Section Test Results

The Marx generator output pulses enter the water insulated section through 36 polyurethane, high voltage feedthroughs. To date, no breakdowns have been observed on these feedthroughs from the 2.5 MV peak voltage with a t_{eff} of 200 nsec, where t_{eff} is the time in which the voltage is greater than 63% of maximum voltage. The water capacitor's inner high voltage electrode is cantilevered from the center of the feedthrough insulator. To date no intermediate store breakdowns have been observed. The SF_6 triggered switch exhibits a prefire probability of about 0.05. Typically, one module's trigatron will discharge its water capacitor between 10 to 50 ns before the trigger pulse arrives. If the trigatron prefires are removed from the data base, the switch synchronization is excellent. The pulse forming lines, line supports, and self-break water switches are operating as expected.

Figure 2 shows the total PBFA-I module jitter we measured at the vacuum interface. The module jitter provides data on the operation of each module's pulse forming network. The total 36 module timing spread is 14 ns which is equivalent to a total single module jitter of 3.7 ± 1 ns. Of the 3.7 ns, our previous tests[2] predict that the expected water switch jitter is 1.6 ns and implies a trigatron gas switch jitter of 3.3 ns. Tests on eight Proto-II[3] switches showed a jitter of 3.5 ns in an operational accelerator. In summary, the overall switching jitter is consistent with our past experience and the PBFA-I design parameters.

One development,[4] which has enhanced the modular pulsed power feasibility is the water polarity reversing convolute. Simply stated, the input ground lines are connected to the output high voltage lines and the input high voltage lines are connected to the output ground lines as shown in Figure 3. Data from PBFA-I, which has half of its lines convoluted, shows the convolutes to be from 90 to 100 percent efficient. With the use of this convolute, particles can be accelerated between either +2 MV or -2 MV and ground or between the +2 MV and -2 MV terminals for a total acceleration potential of 4 MV. PBFA-I was checked out in this alternating polarity configuration. Typical results from two single modules in opposite polarities are shown in Figure 4 where the forward going powers in the water section as a function of time are compared. The positive and negative module outputs are almost identical.

Vacuum Interface -- Magnetically Insulated Transmission Line (MITL) Test Results

The vacuum interfaces, which were designed to withstand 3.5 MV, have operated well with the 2 MV pulse. This overdesign provides reliability and the interfaces have worked well with no flashovers during testing. This overdesign should allow longer time

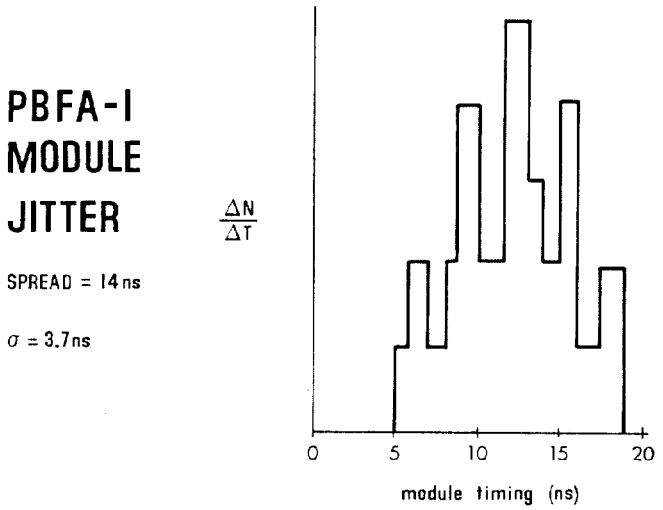

Figure 2. PBFA-I module jitter.

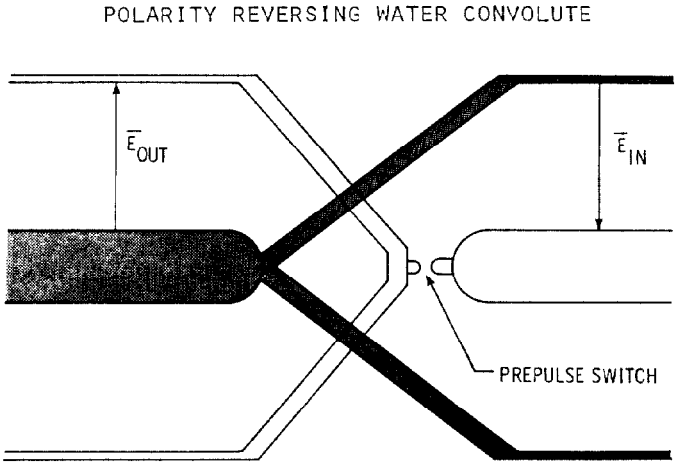

Figure 3. Water convolute.

intervals between cleaning and maintenance.

The MITL's operated well with electron beam diodes for the loads. Data shown previously[5] indicates a transport efficiency of .9.

Output Test Results

A large number of outputs (36) and the resulting instrumentation requirements, make the testing of a modular accelerator a step by step procedure. First, single module shots were made on the Mite and HydraMite accelerators in both polarities and the input and output were measured on the MITL. The output voltage was inferred from multiple current measurements[5,6] while the input voltage was measured. Impedance, voltage, and power, as a function of time at the input and output were obtained. When the MITL load impedance was relatively constant and repeatable, the energy was efficiently transported from the input to the output. All deviations from the efficient transport condition were caused by misalignment and were obvious from the current input monitor to the MITL. For reference, the MITL power inputs for opposite polarity PBFA-I lines are compared

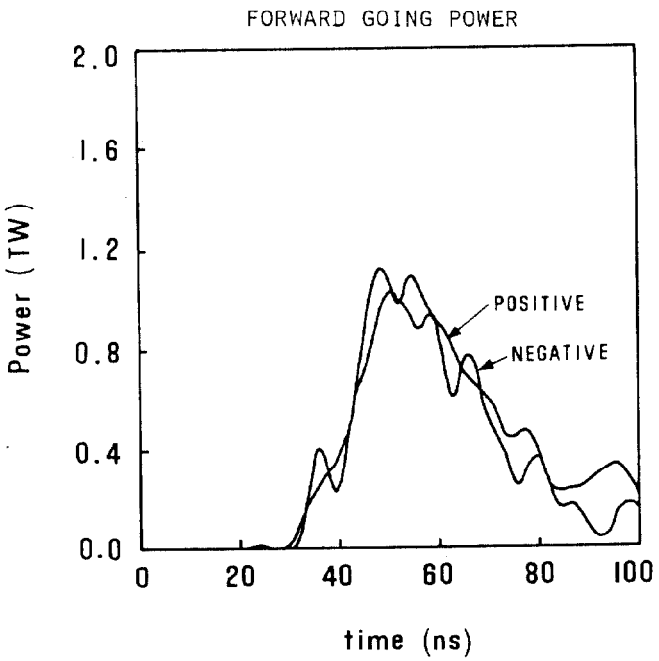

Figure 4. Comparison of forward going power.

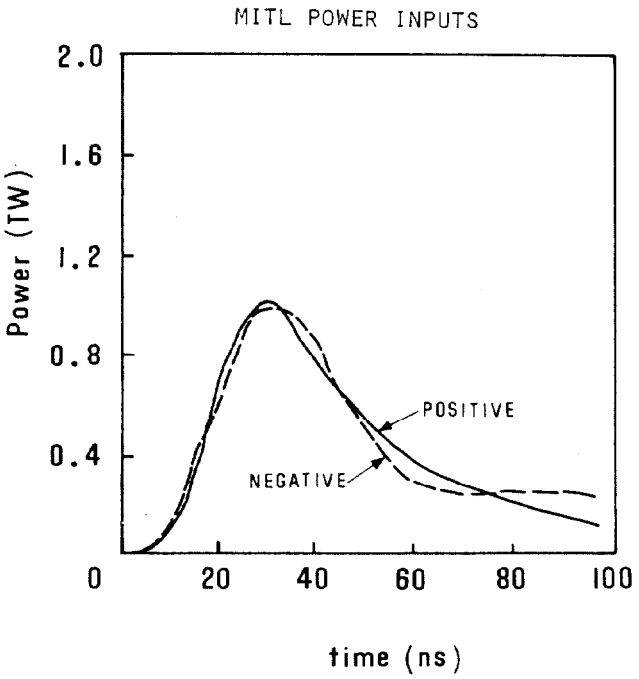

Figure 5. MITL power inputs.

in Figure 5 and show similar characteristics.

Second, any non-standard module switching characteristic or voltage level is observed as a shift in the output time of the module. A unique characteristic of the liquid dielectric is the combined voltage and time dependence of its electrical breakdown strength. This relationship will be derived.

The module output pulse time t_m is determined by the gas switch breakdown time interval t_g plus the water switch breakdown time interval t_w for each module, i.e.,

$$t_m = t_g + t_w \quad .$$

Since the water switches are self-breaking switches, t_w is determined by the applied voltage waveform. The breakdown of a water switch[7] is given by:

$$\frac{V_o}{d} = \frac{0.13}{t_{eff}^{0.5}} \frac{MV}{cm}$$

This t_{eff} equals the time in microseconds during which the voltage is greater than 67% of V_o. The relationship between the variation δt_w in the module timing and the variation δV in the peak voltage is derived.

$$\frac{\delta V}{V_o} = - \frac{\delta t_w}{2\, t_{eff}} \quad .$$

The 36 PBFA-I modules timing data shows the total jitter is 3.7 ns. Consequently δt_w is less than 3.7 ns. The effective charge time t_{eff} is 70 ns, and the rms variation in the module voltage must be less than 2.7%. Consequently, the excellent simultaneity of the module timing necessarily verifies that the pulse forming network was working well. Since the output power is proportional to V_o^2, the standard deviation in module power due to varying voltages is expected to be less than 5.4%.

Third, to ascertain that PBFA was operating at the correct nominal voltages, two PBFA-I modules were instrumented with vacuum interface voltage monitors. The voltage level, the simultaneity and the derived power output were in excellent agreement as was shown in Figure 4.

Fourth, after the PBFA-I module performance was verified to be the same as the prototype module performance, the current monitors were installed as the prime PBFA-I monitor. By using the current into the vacuum interface and the typical MITL impedance (Figure 6) which varies as a function of time, the power into the MITL injector is obtained.

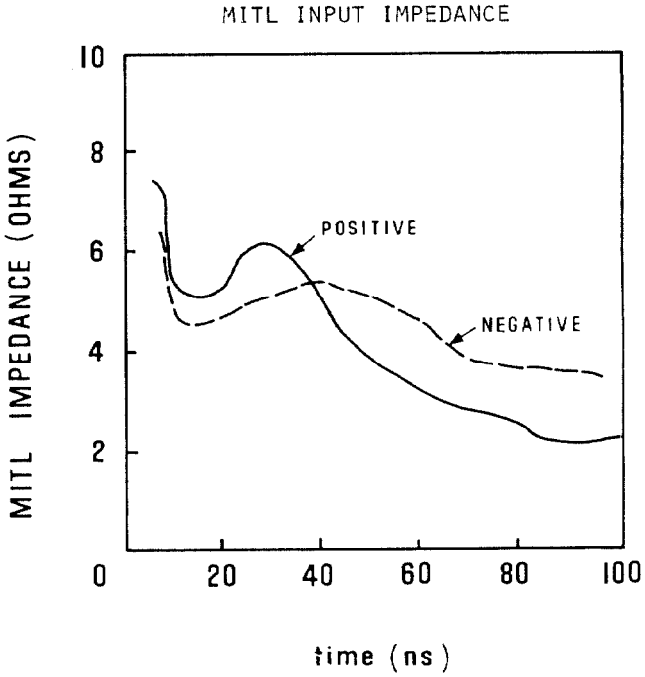

Figure 6. MITL input impedances.

A PBFA power pulse is shown in Figure 7 where the 36 inputs to the MITL are summed, as they arrived, for one shot. The MITL input is the wider pulse while the dotted line shows the expected beam front erosion due to the MITL.[8]

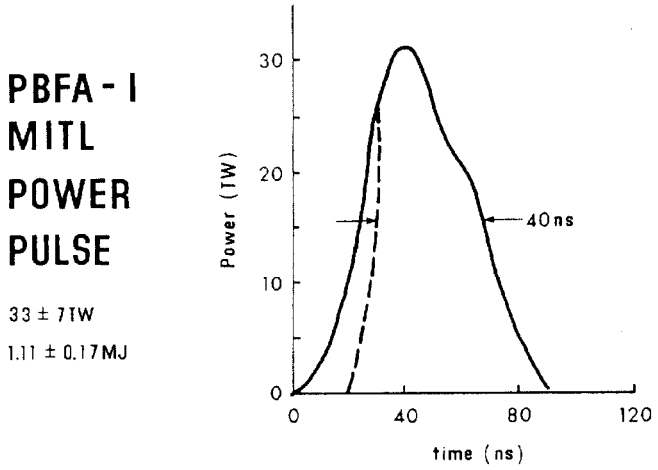

Figure 7. PBFA-I MITL power pulse.

The instrumentation showed the power input to the MITL's and it inferred, by appropriate current traces, that this power was efficiently transported to the load end. Another independent, yet simple, experiment is still desirable to verify the energy transport. A dosimeter measurement of the bremsstrahlung output was used to infer the power at the electron beam diodes. The technique was developed at the Atomic Weapons Research Establishment[9] and has been used at Sandia National Laboratories. The output of each MITL was terminated in an anode-cathode (A-K) gap, which consisted of a dual blade cathode and a carbon block anode. The radiation dose at one point on each of the A-K gap ground planes and at the center of the accelerator was measured with collimated thermo-luminescent detectors. The A-K gaps were set at 1.1 cm, which insured that the effective output impedance was the self-limited MITL impedance of 4.8 ohms. The beams did not pinch, but some fraction of the beams hit the sides of the MITL's in front of the loads. This loss meant that the x-ray dose at the center of the accelerator was reduced. The x-ray dose was then used to infer the total module power and the individual module dose measurements were used to infer the variation between modules.

The dose rate at one meter from the anode of a paraxial electron beam into carbon is given by $\dot{D} = (K)\ I\ V^{2.8}$, where K = 5.4E-15 and the units are in rads, amperes, and volts. For a constant impedance load Z_L, $I = V/Z_L$ so $\dot{D} = K\ V^{3.8}/Z_L$. The power P is proportional to V^2/Z_L, so $\dot{D} = K\ P^{1.9}\ Z_L^{0.9}$. The calculated total dose is given by $D = K P_{max}^{1.9}\ Z_L^{0.9}\ t_{eff}$, where t_{eff} is now defined as

$$t_{eff} = \frac{1}{P_{max}^{1.9}} \int_0^\infty P(t)^{1.9}\ dt$$

which was determined to be 24.5 ns from the analysis of the voltage waveforms in Figure 7. Consequently,

$$P_{max} = \left(\frac{D}{K\ Z_L^{0.9}\ t_{eff}} \right)^{0.526}$$

The measured average dose on axis for the accelerator was 38 rads at one meter. The effective attenuation for the TLD collimators and the anode plates was computed to be 6.5 ± 0.5. The diode current in each module exceeds the critical current for pinching by 60%, so the electron flow is a diffuse pinch with an effective electron half angle of between 15° and 22-1/2°. Consequently, the expected dose on axis at one meter is between 50% and 65% of the dose from a true radial beam. Therefore, the unattenuated dose (D) for the equivalent radial beam is 434 ± 61 rads. The dose from the positive lines was only 3% of that from the negative lines because the radiation was directed radially outward for the positive lines. Consequently, only the eighteen negative lines contributed dose on axis. Z_L = 0.27 ohms or one eighteenth of the self-limited impedance of a single module. Therefore, P_{max} = 14.6 ± 1 TW for the eighteen negative lines or an extrapolated output of 29.2 ± 2 TW for all thirty-six lines. The power transport down the negative MITL's appears to be excellent. A similar analysis of the individual module doses indicate the module power had 14% standard deviation. A more direct measurement of the power and energy at the MITL's loads will be obtained after a new instrumentation system is completed. The present measured timing spreads, powers, and energies are summarized in Figure 8.

PBFA-II Projections

PBFA-II will be a 100 TW accelerator to test breakeven targets. This accelerator will be capable of providing a ± 4 MV, 25 MA, 40 nsec, 3.5 MJ output pulse. It uses 72 upgraded Marx generators with each providing a 210 kJ energy store capability in the same module size as the 112 kJ, PBFA-I Marx. The number of pulse forming lines per module will be increased from two to four. A series of convolutes will double the voltage using voltage vector inversion principles.[4]

PBFA-I Data Summary

Shot	No. Data Collected	P_{MITL}	W_{MITL}	Module Spread	P_{TLD}
178	32	28. ± 6 TW	1009 ± 147 kJ	13 ns	----
179	27	29.3 ± 6 TW	941 ± 111 kJ	15 ns	----
184	32	33.3 ± 6.6 TW	1109 ± 166 kJ	13 ns	27.3
186	34	29. ± 5.2 TW	980 ± 134 kJ	24 ns	30.6
187	34	29.6 ± 5.8 TW	1042 ± 147 kJ	14 ns	29.0

Figure 8. Data summary for PBFA-I five shot series.

A higher voltage diode and MITL will conduct the ± 4 MV pulses into a central chamber where they will be combined by a magnetic convolute to provide either a 4 or 8 MV acceleration capability.

Conclusion

PBFA-I has essentially demonstrated its predicted output parameters of 30 TW, 2 MV, 1 MJ output in a modular, extendable accelerator. It is now entering its operational phase and will provide a useful test bed. PBFA-I has proven that a 100 TW, 3.5 MV, PBFA-II accelerator is feasible with the modular approach.

References

1. D. L. Johnson, Initial Proto-II Pulsed Power Tests, Proceedings of the International Pulsed Power Conference, November 1976, p. 1E2-1.

2. D. L. Johnson, J. P. VanDevender, and T. H. Martin, IEEE Transactions on Plasma Science, PS-8, No. 3, 204 (1980).

3. T. H. Martin, D. L. Johnson, and D. H. McDaniel, Super Power Generators, Proceedings of the 2nd International Topical Conference on High Power Electron and Ion Beam Research and Technology, V. II, Ithaca, New York, October 1977.

4. T. H. Martin, J. P. VanDevender, G. W. Barr, and D. L. Johnson, EBFA--Pulsed Power for Fusion, ISI Proceedings of the 3rd International Topical Conference on High Power Electron and Ion Beams, July 1979, Novosibirsk, USSR.

5. J. P. VanDevender, Long Magnetically Insulated Power Transport Experiments, J. Appl. Phys. 50 (6), June 1979.

6. C. W. Mendel, Jr., J. P. VanDevender, and G. W. Kuswa, Proceedings of the International Pulsed Power Conference, June 1979, p. 153.

7. J. P. VanDevender and T. H. Martin, Untriggered Water Switching, IEEE Transactions on Nuclear Science, Vol. NS-22, No. 3, June 1975.

8. D. H. McDaniel, J. W. Poukey, K. D. Bergeron, J. P. VanDevender, and D. L. Johnson, Power Flow Studies of Magnetically Insulated Lines, Proceedings of the 2nd International Topical Conference on High Power Electron and Ion Beam Research and Technology, V. II, Ithaca, New York, October 1977.

9. D. W. Forster, M. Goodman, G. Herbert, J. C. Martin, and T. Storr, Electron Beam Diagnostics Using X-Rays, AWRE Report SSWA/JCM/714/162, Aldermaston, England (1971).